RSC Advances

ROYAL SOCIETY OF CHEMISTRY

www.rsc.org/advances

Design of a strong-base anion exchanger and its adsorption and elution behavior of rhenium (VII)

Jianhua Zu,[*a] Maosong Ye, [a] Puyin Wang,[a] Fangdong Tang[b] and Linfeng He[b]

[a]*School of Nuclear Science and Engineering, Shanghai Jiao Tong University, Shanghai 200240, China*

[b]*Shanghai Institute of Measurement and Testing Technology, Shanghai 201203, China*

Correspondence to: Jianhua Zu (E-mail: zujianhua@sjtu.edu.cn)

A novel strong-base anion exchanger (PS-g-4VP-IE) is prepared by γ-irradiation-induced grafting of 4-vinyl pyridine onto polystyrene microspheres, followed by quaternization process. The effects of absorbed dose and monomer concentration on grafting yield, and quaternization time on conversion ratio were investigated in order to obtain optimum synthesis conditions. The ATR-FTIR and XPS results effectively manifest the successful synthesis of PS-g-4VP-IE. Furthermore, the effect of solution acidity on adsorption efficiency, adsorption kinetics and adsorption isotherm were investigated in batch wise experiments. The results reveal that the adsorption towards perrhenate (ReO_4^-) not only have rather fast adsorption kinetics, but also match well with the Langmuir isotherm model. Thus, its theoretical maximum adsorption capacity is deduced to be 252 mg g^{-1}, while the couterpart is 247 mg g^{-1} in column experiments. The concentrated elution peak shows the potential application of PS-g-4VP-IE in concentrating ReO_4^-.

1. Introduction

Rhenium (Re) is one of the least-abundant elements on the earth whose abundance in the earth's crust is merely 10^{-7}%. However, there is a wide application of Re in chemical engineering, metallurgy, national defense, radiopharmaceuticals and so on. Therefore, in recent years, the research

of concentrating Re (VII) which is the most stable oxidation valence of Re,[1] has attracted increasingly great attention, where extraction[2,3] and ion exchange[4,5] are the two most popular methods.

Nevertheless, extraction has its own defects such as slow kinetics, toxic extraction solvent resulting in secondary waste which is difficult for treatment and disposal.[6] On the contrary, ion exchange has overcome these drawbacks because of its other advantages over extraction such as regeneration ability and low cost. Therefore, a variety of ion exchange membranes,[7]powdery resins which contained amino groups in their molecular structures had been developed. For instance, in 2004, Kim et al. demonstrated that natural organic polymer chitosan, containing amino groups, was able to absorb perrhenate (ReO_4^-) effectively.[8] Yeon-Sung Chung et al. prepared a powdery anion exchanger functionalized with quaternary ammonium groups and used them for the adsorption of ReO_4^- from aqueous solution.[9] Lan et al used a gel type resin 201×7 for the recovery of Re(Ⅶ) from a molybdenite calcine and Lukic et al. used Dowex1-x8 for the adsorption of Re(Ⅶ) from dilute sodium chloride solutions.[10,11] The above strongly basic anion exchange resins which contain alkylamino had poor stability against radiation or high acidity.[12] Furthermore, all these materials were not suitable for column application due to their poor mechanical stability or high pressure drop.[13]

Thus, it gave rise to the synthesis of microsphere-type anion exchangers which has good performance and high stability.[14] To meet these demands, polystyrene microspheres (PS) can be a wise choice for substrates due to its ideal size and hardness. Moreover, other obvious advantages such as low cost and the ease of production also have rendered PS a commercially successful and easily accessible product in industry. On the other hand, compared with chemical modification of

substrates which will produce more pollution problems, radiation-induced grafting technique has unique advantages such as more easily controllable and using less toxic chemical reagents due to fewer synthesizing procedures.

As a consequence, in our work, using PS as substrates, 4-vinyl pyridine (4-VP) as monomer, and iodoethane as quaternization reagent, we successfully synthesized a novel strong-base anion exchanger (PS-g-4VP-IE) by means of radiation-induced grafting technique. By changing grafting and quaternizaton conditions, we can obtain anion exchanger with different ion exchange capacity. Then, through both batch wise and column experiments, we tested its adsorption and elution properties towards rhenium (VII) and expected its potential for future application in concentrating rhenium.

2. Experimental

2.1 Materials

Polystyrene microspheres (PS) were purchased from Shanghai resin factory Co., Ltd. (average diameter: 350μm). 4-vinyl pyridine (4-VP, purity>95%) stabilized with hydroquinone and ammonium perrhenate (purity>99%) were purchased from Sigma-Aldrich. Iodoethane and nitric acid were all obtained from Sinopharm Chemical Reagent Co., Ltd. All reagents were used without further purification.

2.2 Preparation of PS-g-4VP-IE

The preparation procedures of PS-g-4VP-IE are shown in Fig. 1 in which simultaneous irradiation grafting method was employed.

2.2.1 Preparation of graft copolymer PS-g-4VP by simultaneous irradiation grafting method

Different amount of 4-VP (as monomer) were mixed with dioxane (as solvent), then an

appropriate amount of hydroquinone (as polymerization inhibitor which could help avoid homopolymerisation properly and reduce the viscosity of grafting copolymerization system) were added into the solution. After 15 min of bubbling with nitrogen, a preweighed amount of PS was immersed in the mixture of 4-VP and the solvent, the mixture was deaerated by 5 min of bubbling with nitrogen in order to eliminate oxygen. Then the sealed glass bottles were irradiated under γ-ray in different doses. After irradiation, the graft copolymer was purified by Soxhlet extraction under 78℃ for 24 h where the mixture of ethanol and water (1:1) were used as medium. Lastly, after dried in a vacuum oven at 50℃ for 72 h, the graft copolymer was weighed again. The grafting yield (%) was determined by the percentage increase of weight. The formula is described as:

$$\text{Grafting yield (\%)} = \frac{W_g - W_0}{W_0} \times 100 \qquad (1)$$

where W_g and W_0 (g) are the weights of grafted and initial polystyrene microspheres, respectively.

2.2.2 Preparation of PS-g-4VP-IE by quaternization of PS-g-4VP

Quaternization process was carried out as followed. Firstly, we allowed some PS-g-4VP graft copolymer to swell in trichloromethane in a fume hood so that the trichloromethane would absolutely volatize after 24 h and the PS-g-4VP got adequately swollen. Then PS-g-4VP was refluxed in the mixture of excess iodoethane and ethanol (as solvent) in a three-necked flask with constant stirring under the temperature of 70℃ for different time. The resulting PS-g-4VP-IE were purified by washing with ethanol and distilled water, and dried in a vacuum oven at 50℃ for 72 h. The conversion ratio (%) was calculated by:

$$\text{Conversion ratio (\%)} = \frac{W_a - W_g}{W_g - W_0} \times \frac{M_1}{M_2} \times 100 \qquad (2)$$

where W_a (g) stands for the weight of quaternized PS-g-4VP, M_1 and M_2 (g mol^{-1}) stand for the molecular weight of 4-VP and iodoethane, respectively.

2.3 Characterization of PS-g-4VP-IE

2.3.1 FTIR analysis

Structrural analysis of the PS, PS-g-4VP and PS-g-4VP-IE were performed by FTIR spectroscopy (IR Affinity-1, Shimadzu). The spectra were measured in range of 650 cm^{-1} to 4000 cm^{-1}.

2.3.2 XPS analysis

XPS analysis of total elements and N element of PS-g-4VP and PS-g-4VP-IE were carried out by an ESCALAB 250 Xi instrument from Thermo Fisher using monochromatic Al Kα radiation (225 W, 15 mA, 15 kV) and low energy electron flooding for charge compensation. To compensate for surface charges effects, binding energies (BE) were calibrated using C_{1s} hydrocarbon peak at a BE of 284.80 eV. The data were exported into VAMAS file format and imported into CASA XPS software package for manipulation and curve fitting.

2.4 Batch wise experiments

The effects of solution acidity on adsorption efficiency were carried out by adding 0.1 g PS-g-4VP-IE and 5 ml solution of ammonium perrhenate (100 mg l^{-1}) with various acidity values which were adjusted by HNO_3 into a 12ml glass bottle. Then the sealed bottles were vibrated in water-bath shaker (NTS-4000C, Tokyo Rikakikai Co., LTD) at the rate of 120 rpm for much longer than equilibrium time at room temperature. The concentration of rhenium was measured by an inductively coupled plasma atomic emission spectrometer (ICPS-7510, Shimadzu). The adsorption efficiency (%) was determined by:

$$\text{Adsorption efficiency (\%)} = \frac{C_0 - C_e}{C_0} \times 100 \qquad (3)$$

where C_0 and C_e (mg l^{-1}) are the initial and residual concentration of rhenium at equilibrium time in

solution, respectively.

Other studies including the maximum adsorption capacity, adsorption kinetics and temperature influence on the adsorption behavior of PS-g-4VP-IE were all carried out in similar approaches. The adsorption capacity (Q, mg g^{-1}) was calculated by:

$$Q = (C_0 - C_e) \times \frac{V}{m} \quad (4)$$

where V (ml) is the volume of the feed solution and m (g) is the mass of dry PS-g-4VP-IE.

2.5 Column experiments

Under room temperature, the solution of ammonium perrhenate (C_0=1200 mg l^{-1}) was pumped through a fixed-bed column (Φ=5 mm, H=50 mm) which was compacted with 0.8 g PS-g-4VP-IE. The flow rate was set at averagely 0.28 ml min^{-1}. The effluent was collected in tubes every 10min and the concentration of rhenium in each tube was measured by ICP. The saturated adsorption capacity (Q_m, mg g^{-1}) was calculated through the integral value of the adsorption curve.

After column adsorption experiments, firstly, enough distilled water was pumped through the column to clean the residual Re attached to the column walls other than absorbed by PS-g-4VP-IE. Then, 5M HNO_3 was pumped through the above column in which the strong base anion exchanger has reached its saturated adsorption capacity. The effluent was collected every 5 min in tubes while the flow rate was still set at 0.28 ml min^{-1}. The concentration of Re in tubes was measured by ICP. The eluted amount of Re was calculated via the integral value of the elution curve.

3. Results and discussion

3.1 Preparation of PS-g-4VP-IE

The effect of absorbed dose and monomer (4-VP) concentration on grafting yield was investigated (Fig. 2). In Fig. 2 (a), when the monomer concentration is 20 wt %, the grafting yield

rises with the increase of absorbed dose and then levels off after 20 kGy. The grafting reaction depends largely on concentration of the trapped radicals available to monomers within PS microspheres. Higher is absorbed dose, and more trapped radicals is available to the 4-VP monomer. With further increase of absorbed dose, a large amount of homopolymer will be formed at a high absorbed dose,[15] which reduces the diffusion rate of monomers. As a result, the grafting yield almost levelled off when absorbed dose was higher than 20 kGy. Meanwhile, in Fig. 2 (b), where absorbed dose is fixed at 30 kGy, the grafting yield rises rapidly with the increase of monomer concentration. However, due to increasing monomer concentration which results in difficulty in getting rid of homopolymer, the irradiation condition 30 kGy was selected as absorbed dose and 25 vol % as monomer concentration. Thus, the sample with grafting yield 63.4 % was used to react with iodoethane.

On the second hand, the effect of quaternization time accounting for the conversion ratio was also investigated. The obvious trend in Fig. 3 indicates that 48 h are enough for quaternization, and the resulting conversion ratio has reached above 95%. Because ion exchange capacity is controlled by conversion ratio, the quaternization conditions are every important for improving the maximum adsorption capacity of PS-g-4VP-IE and its adsorption kinetics.[16-19] Thus, in the following experiments, PS-g-4VP-IE with 63.4% grafting yield and 96.5% conversion ratio were used for adsorption or elution.

3.2 ATR-FTIR analysis

Firstly, FTIR analysis was employed to investigate the structural changes after grafting and quaternization process, respectively. Fig. 4(a) shows the FTIR spectra of PS, in which the characteristic adsorption peaks at 1490 and 1600 cm^{-1} correspond with the aromatic C=C in-plane

stretching vibration of benzene ring; And the strong adsorption peaks at 696 and 760 cm^{-1} are attributed to the aromatic C-H deformation of substituted benzene ring;[20] Compared with Fig. 4(a), the adsorption peak at 1556 cm^{-1} in Fig. 4(b) is assigned to the C=N stretching vibration of pyridine ring; and the appearance of adsorption peak at 1415 cm^{-1} is assigned to the C=C stretching vibration of pyridine ring.[21] These two changes are shown as direct evidence for the successful graft of 4-VP onto PS. Moreover, in Fig. 4(c), along with weakness of the adsorption peak at 1556 and 1600 cm^{-1}, the emergence of adsorption peak at 1640 cm^{-1} indicate that nitrogen atoms in pyridine rings were positively charged.[22] Therefore, the quaternization process was also proved to be effective.

3.3 XPS analysis

For further verification of successful synthesis of PS-g-4VP-IE, XPS analysis was also employed. The XPS spectra of total elements and N element of samples before (a) and after (b) quaternization were shown in Fig. 5(A) and 5(B). Both samples show two characteristic peaks at binding energy of 282.08 eV and 397.08 eV in Fig. 5(A) which correspond to C_{1s} and N_{1s}, respectively. The emergence of peak at 616.08eV, which corresponds to I_{3d}, can be attributed to the quaternization reagents, iodoethane. Compared Fig. 5B (b) with Fig. 5B (a), the apparent peak splitting of N_{1s} can be regarded as a signal from the positively charged nitrogen, further confirming the successful quaternization reaction.

3.4 Batch wise experiments

3.4.1 The effect of solution acidity

In order to apply PS-g-4VP-IE into practical use, it is meaningful for us to study the effect of solution acidity on the anion exchanger's adsorption efficiency, which would also offer some hints for its elution behavior in return. As plotted in Fig. 6, the adsorption efficiency increases rapidly with

the decrease of acidity till the acidity value ($-\log C_{HNO_3}$) is greater than 2.59 where the adsorption efficiency has reached above 97%. In extreme acidity where the acidity value is -0.69 (corresponding with 5M HNO_3), the adsorption efficiency is merely 6.5%, which can be explained by the strong competition of NO_3^- against ReO_4^- for the quaternary amine groups onto PS-g-4VP-IE. Here in this work, in order to reach the maximum efficiency, the following adsorption experiments were performed in solution without HNO_3, corresponding with the acidity value of 6.4.

3.4.2 The adsorption kinetics

The investigation of equilibrium time before anion exchanger reaching its maximum capacity is of great significance for the study of adsorption mechanism of PS-g-4VP-IE. Therefore, the relationship between time (t) and adsorption capacity (Q) under different temperatures was shown in Fig. 7(A). The adsorption capacity ascends rapidly within 30 min, and then reaches equilibrium. These experimental results indicate that PS-g-4VP-IE has rather fast adsorption kinetics.[23] Therefore, in the subsequent experiment, 2 h is chosen as equilibrium time in order to achieve the saturated adsorption capacity.

In addition, both pseudo-first-order and pseudo-second-order kinetic models (Eq. (5) and (6)) were applied to fit the adsorption kinetic datum.

$$-\ln(1-F) = K_1 t\ ,\quad F = \frac{Q_e - Q_t}{Q_e} \qquad (5)$$

$$\frac{t}{Q_t} = \frac{1}{K_2 Q_e^2} + \frac{1}{Q_e} t \qquad (6)$$

where Q_e and Q_t (mg g^{-1}) are the calculated amounts of Re (VII) absorbed by per unit dry PS-g-4VP-IE at equilibrium and at time t (min); K_1 and K_2 are the rate constant for the pseudo-first-order and pseudo-second-order model.

The experimental results, as shown in Fig. 7(A), can be converted into the plot -ln(1-F) and t/Q_t

versus t in Fig. 7(B), correspondingly. However, in Fig. 7(B), the correlation coefficient (R^2) of line b is much low than line a (at room temperature, 0.745 versus 0.999), which means the adsorption process matched much better with pseudo-second-order than pseudo-first-order model. Therefore, K_2 and Q_e obtained from the intercept and slope is 0.018 min^{-1} and 90.5 mg g^{-1}. K_2 is high than the value of 0.0165 min^{-1} reported by Jia et. al when N-methylimdazolium functionalized strong basic anion exchange resin was used for adsorption and separation of Re (VII). [24] The theoretical Q_e corresponds well with experimental Q_e shown as Fig. 7(A), which is 89.9 mg g^{-1}. Furthermore, because of Q_e converging to the very similar value in Fig. 7(A) under various temperatures, indicating that the adsorption kinetics of PS-g-4VP-IE is hardly dependent on temperature. Therefore, 25℃ is chosen for further experiments.

3.4.3 Adsorption isotherm

The adsorption isotherm of PS-g-4VP-IE at room temperature is shown in Fig. 8(a). Combining the isotherm with Langmuir isotherm model which is effective for studying homogeneous and monolayer adsorption onto a surface with a finite number of identical sites,[25] we can figure out the theoretical maximum adsorption capacity (Q_m, mg g^{-1}).

$$\frac{C_e}{Q_e} = \frac{C_e}{Q_m} + \frac{1}{K_L Q_m} \qquad (7)$$

where K_L (l g^{-1}) stands for the adsorption energy.

In Fig. 8(a), the initial concentration of Re (VII) ranges from 2000 to 5000 mg l^{-1}. The correlation coefficient of Langmuir plot presented in Fig. 8(b) is 0.990, which indicates that the adsorption process fits with the Langmuir isotherm model. In return, via the slop ($1/Q_m$) of the plot, the theoretical maximum adsorption capacity was calculated to be 252 mg g^{-1}. Q_m is higher than bio-char produced from Acidosasa edulis shoot shell (14.6 mg g^{-1}) and lower than N-methylimidazolium

functionalized strongly basic anion exchanger (351.4 mg g^{-1}). [26,27]

3.5 Column experiments

3.5.1 Adsorption of Re (VII)

Column experiment is another way for judging the adsorption behavior of an anion exchanger because large-scale utilization usually includes column application. Therefore, the column adsorption experiment of PS-g-4VP-IE was performed firstly, and the break-through curve is depicted in Fig. 9(A). The result shows the relative Re concentration (the ratio of Re concentration in effluent to that in feed solution) with the feed solution bed volume. After the first 150 bed volumes, there are almost no appearance of Re in the effluent. Then, the concentration of Re in effluent increases till 230 bed volumes which indicates the loaded anion exchanger had reached saturated adsorption capacity. Through integral value of this break-through curve, the maximum adsorption capacity in column experiments was calculated to be 247 mg g^{-1}. This value is in good agreement with 252mg g^{-1} which was determined via Langmuir isotherm adsorption model in batch wise experiments, which indicates PS-g-4VP-IE has a good performance in column adsorption experiment.

3.5.2 Elution of Re (VII)

After column adsorption experiment of Re (VII) onto PS-g-4VP-IE, its elution behavior, an important criterion for judging an anion exchanger in column application as well, was evaluated. Therefore, in avoid of introducing other metal ions, inferring from the acidity dependence of adsorption behavior of the PS-g-4VP-IE in batch wise adsorption experiment, we selected 5M HNO_3 as eluent. In Fig. 9(B), the Re concentration decreases drastically within the first 30 bed volumes where nearly 89% of Re (in 230 bed volumes) was eluted. The results show that Re（VII）can be concentrated almost 8 times after elution. Moreover, the maximum amount of eluted Re can reach up

to 95% in 60 bed volumes, which, in return, manifests the potential application of PS-g-4VP-IE in concentrating Re.

4. Conclusions

A novel strong-base anion exchanger, PS-g-4VP-IE, was synthesized by radiation-induced grafting of 4-VP onto the substrates, polystyrene microspheres, and further quaternized by iodoethane. The highest grafting yield 96% was achieved with 30 kGy absorbed dose at 25 vol % of 4-VP diluted with dioxane. The maximum conversion ratio 96.5% was obtained when PS-g-4VP graft copolymer reacted with iodoethane for 48h at 70℃. ATR-FTIR analysis and XPS spectra were all shown as evidences for successful grafting and quaternizaton reactions. PS-g-4VP-IE with 63.4% grafting yield and 96.5% conversion ratio was applied as an effective anion exchanger in batch wise and column experiments. The equilibrium adsorption capacity of PS-g-4VP-IE is hardly affect by temperature and high adsorption capacity for Re (VII) is obtained over a wide pH range from 1.5-6.4. In batch wise experiments, PS-g-4VP-IE showed comparatively faster adsorption kinetics which matched well with pseudo-second-order model. Through Langmuir isotherm adsorption model, the maximum adsorption capacity was worked out to be 252 mg g^{-1}. In column experiments, PS-g-4VP-IE showed an ideal performance both in adsorption and elution process. Absorbed Re（VII）can be concentrated almost 8 times after elution. Therefore, PS-g-4VP-IE can be regarded as a competitive candidate in the future research of concentrating Re (VII).

Acknowledgements

Financial support from the National Natural Science Foundation of China (Grand No. 91226111 and 11305102) and Shanghai Science and Technology Foundation (Grand No. 12DZ2293800) are gratefully acknowledged.

References

1. M. C. Chakravorti, *Coord. Chem. Rev.,* 1990, **106**, 205-225.
2. Z. F. Cao, H. Zhong and Z. H. Qiu, *Hydrometallurgy,* 2009, **97**, 153-157.
3. D. W. Fang; X. J. Gu and Y. Xiong, *J. Chem. Eng. Data.,* 2010, **55**, 4440-4443.
4. N. Nebeker and J. B. Hiskey, *Hydrometallurgy,* 2012, **125-126**, 64-68.
5. A. G. Kholmogorova, O. N. Kononovab, S. V. Kachinb, S. N. Ilyicheva, V. V. Kryuchkova, O. P. Kalyakinab and G. L. Pashkov, *Hydrometallurgy,* 1999, **51,** 19-35.
6. I. A. Miniakhmetov, S. A.Semenov, V. Y. Musatova, *Russ. J. Inorg. Chem*., 2013, **58**, 1380-1382.
7. N. Lamba, Z. V. P. Murthy and R. Kumar, *Sep. Sci. Technol*., 2002, **37,** 191-202.
8. E. Kim, M. F. Benedetti and J. Boulegue, *Water Res.,* 2004, **38,** 448-454.
9. B. Lee, L. L. Bao, H. J. Im, S. Dai, E. W. Hagaman and J. S. Lin, *Langmuir*., 2003, **19,** 4246-4252.
10. X. Lan, S. Liang and Y. Song, *Hydrometallurgy,* 2006, **82**,133-136.
11. D. M. Lukic, J. L. Vucina, and S. K. Milonjic, *J. Serb. Chem. Soc.,* 2008, **73**, 333-339.
12. K. Pillay, J. Radioanal. Nucl. Chem., 1986, **102,** 247-268.
13. Y. S. Chung, B. Lee, K. H. Choo and S. J. Choi, *J. Ind. Eng. Chem.,* 2011, **17,** 114-119.
14. Y. W. Zhang, L. Xu, L. Zhao, J. Peng, C. C. Li, J. Q. Li and M. L. Zhai, *Carbohydr. Polym.,* 2012, **88,** 931-938.
15. L. Xu, J. Sun and L. Zhao, *Radiat. Phys. Chem.,* 2011, **80,** 1268-1274.
16. I. H.Yoon, X. G. Meng, C. Wang, K. W. Kim, S. Bang, E. Choe and L. Lippincott, *J. Hazard. Mater.,* 2009, **164,** 87-94.
17. P. V. Bonnesen, G. M. Brown, S. D. Alexandratos, *Environ. Sci. Technol.,* 2000, **34,** 3761-3766.

18. B. H. Gu, Y. K. Ku and G. M. Brown, *Environ. Sci. Technol.,* 2005, **39,** 901-907.

19. B. H. Gu, G. M. Brown and C. C. Chiang, *Environ. Sci. Technol.,* 2007, **41**, 6277-6282.

20. Z. B. Zhang and C. L. McCormick, *J. Appl. Polym. Sci.,* 1997, **66**, 307-317.

21. N. Sahiner and A. O. Yasar, *J. Colloid. Interf. Sci.,* 2013, **402,** 327-333.

22. S. Maurya, S. H. Shin, K. W. Sung and S. H. Moon, *J. Power Sources,* 2014, **2555,** 325-334.

23. Z. N. Shu and M. H.Yang, *Chin. J. Chem. Eng.,* 2010, **18,** 372-376.

24. M. Jia, H. M. Cui, W. Q. Jin, L. L. Zhu, Y. Liu and J. Chen, *J. Chem. Technol. Biotechnol.,* 2012, **88,** 437-443.

25. M. L. Zhai, M. Wang, L. Xu, J. Peng, J. Q. Li and G. S. Wei, *J. Hazard. Mater.,* 2009, **171**, 820-826.

26. H. Hu, B. Q. Jiang, J. B. Zhang and X. H. Chen, *RSC Adv*., 2015, **5**, 104769-104778.

27. V. Neagu, E.Avram and G. Lisa, *React. Funct. Polym*., 2010, **70**, 88-97.

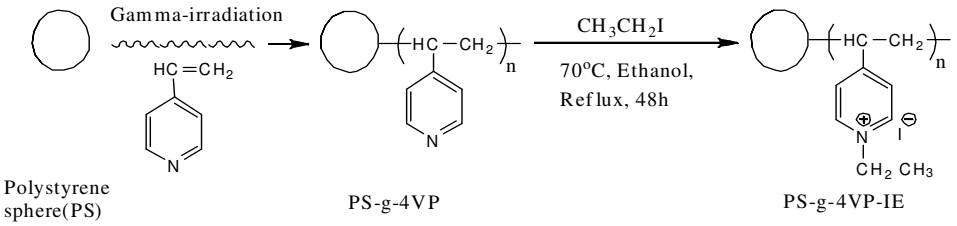

Fig. 1 Synthetic route of PS-g-4VP-IE

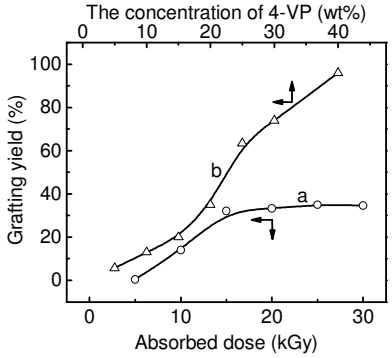

Fig. 2 Effects of absorbed dose (a) and monomer concentration (b) on grafting yield

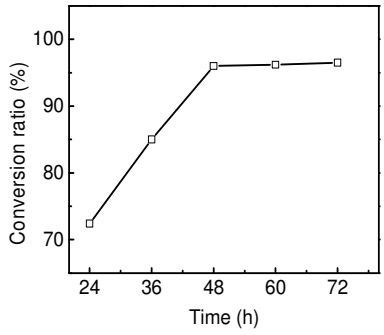

Fig. 3 Effect of quaternization time on conversion ratio

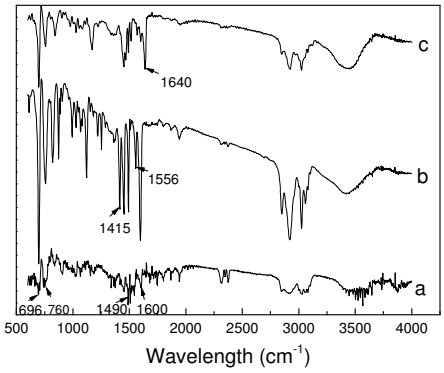

Fig. 4 FTIR spectra of PS (a), PS-g-4VP (b), and PS-g-4VP-IE (c)

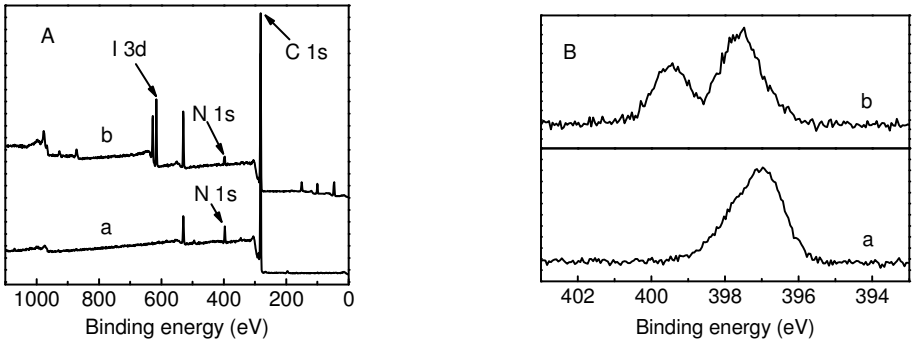

Fig. 5 XPS survey scanning spectra (A): PS-g-4VP (a) and PS-g-4VP-IE (b);

N 1s scanning spectra (B): PS-g-4VP (a) and PS-g-4VP-IE (b).

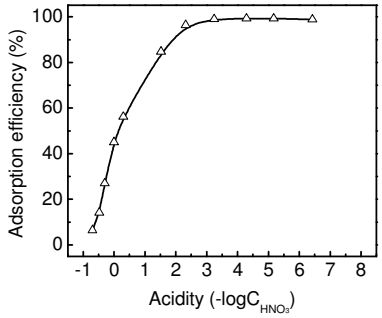

Fig. 6 Effect of solution acidity on adsorption efficiency (C_0: 100mg l^{-1},

solution volume: 5ml, anion exchanger: 0.1g, adsorption time: 2h,

temperature: 25℃)

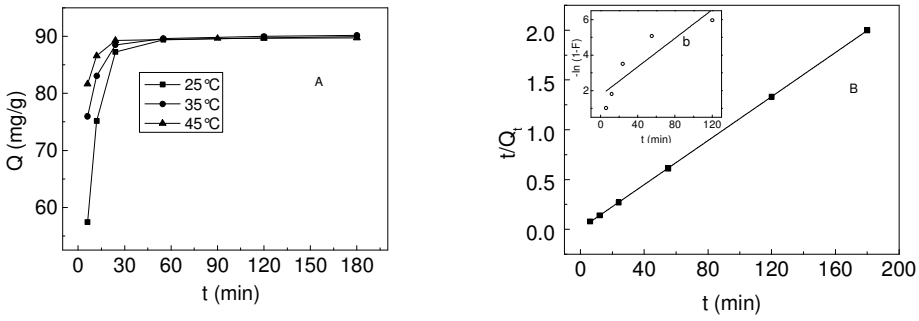

Fig. 7 Kinetics study of adsorption process (A) and kinetic model plot (B): pseudo-first-order kinetics (a) and pseudo-second-order kinetics (b). (C_0: 2000mg l^{-1}, solution volume: 5ml, anion exchanger: 0.1g)

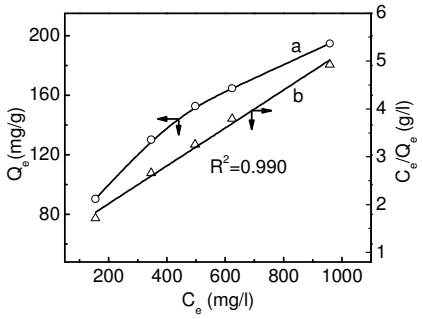

Fig. 8 Adsorption isotherm of Re (VII) on PS-g-4VP-IE (a) and Langmuir linear plot (b), (C_0: 2000-5000mg l^{-1}, anion exchanger: 0.1g, solution volume: 5ml, adsorption time: 2h)

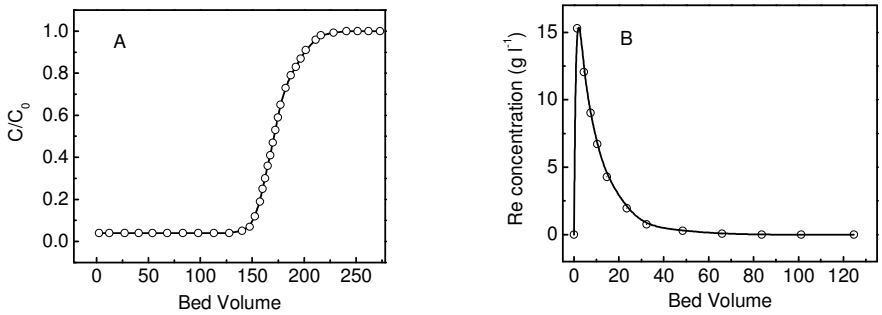

Fig. 9 Rhenium adsorption curve (A) and elution curve (B) on PS-g-4VP-IE from fixed-bed column experiments (C_0: 1200mg l^{-1}, temperature: 25℃)

Graphical abstract

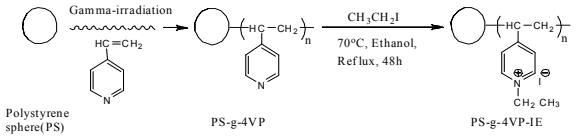

Synthetic route of novel strong-base anion exchanger PS-g-4VP-IE

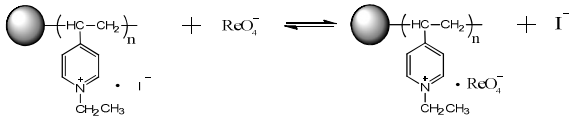

Strong-base anion exchanger reaction with perrhenate